Research Article – Vol. 02, Issue 01, No. 09

Advanced in Engineering and Intelligence Systems

Journal Web Page: https://aeis.bilijipub.com

Exergy, energy, economic, and environmental assessment of gas condensate stabilization units for the selection of optimum configuration

Van Vang Le[1] , Elizabeth C. Matsui[2,*]

[1] *The Ho Chi Minh City University of Transport, Ho Chi Minh City, Viet Nam*
[2] *Dell Medical School, the University of Texas at Austin, Austin, Texas*

Highlights

- Comparative analysis of different gas condensate stabilization units
- Performing energy, exergy, economic, and environmental analyses for all structures.
- Stabilizer column without condenser and with side reboiler has the highest exergy efficiency.
- it is determined that the STB-E is the only structure that can maintain the quality of RVP.

Article Info

Received: 21 February 2023
Received in revised: 27 March 2023
Accepted: 27 March 2023
Available online: 28 March 2023

Keywords

Gas condensate,
Stabilizer column,
Exergy analysis, Simulation,
Economic analysis

Abstract

In this paper, five structures for gas condensate stabilization are simulated and analyzed from the energy, exergy, economic and environmental points of view. These structures are simulated using Aspen HYSYS and Peng-Robinson fluid package. The studied structures are stabilizer column with reboiler and condenser and without preheating (STB-A), stabilizer column with reboiler and without condenser (STB-B), stabilizer column with reboiler, without condenser and with preheating (STB-C), stabilizer column with reboiler, condenser and preheater (STB-D), and stabilizer column with reboiler, without condenser and with side reboiler (STB-E). Exergy efficiency, total production cost, reboiler energy, and total CO_2 emission are calculated for all the structures and compared. According to the performed analysis, STB-E with exergy destruction of 681.9 kW has the highest exergy efficiency (36.37%) among all the studied structures. In addition, technical assessment showed that the STB-C has the highest loss of hydrocarbons through the overhead vapors of the stabilization column. Based on the economic analysis it is deduced that the values of total production costs in STB-C, STB-D, and STB-E are 7.14% lower than the total production costs values of the structures without integration (STB-A and STB-B). Finally, it is determined that the STB-E is the only structure that can maintain the quality of RVP (8 psia) for the produced condensate while simultaneously controlling all the technical, economic and, environmental parameters at desirable levels.

Nomenclature

P	Pressure [kPa]	**Subscript and abbreviations**	
T	Temperature [,^{0} C]		
T_R	Temperature of reboiler[,^{0} C]	RVP	Reid Vapor Pressure
TPC	Total Production cost ($\frac{USD}{kg}$)	NGL	natural gas liquids
TAC	Total Annual cost ($\frac{USD}{year}$)	LPG	liquefied petroleum gas
T_C	Temperature of Condenser [,^{0} C]	IGTC	Ilam Gas Treating Company

* Corresponding Author: Elizabeth C. Matsui
Email: elizabeth.matsui@utexas.edu

T_0	Ambien Temperature[,^{0} C]	VTF	vapor to feed
w_{min}	Minimum Work For Separation	VOC	Variable Operating cost
$\dot{G}_{Feed}$	inlet feed	FOC	Fixed Production cost
$\dot{Q}_R$	net duty of reboiler	$APEA$	Apsen Process Economic Analyzer
$\dot{Q}_C$	net duty of condenser	CRF	Capital Recovery Factor
$\dot{E}_D^{STB}$	total exergy destruction of the stabilizer column	RTO	Real-Time optimization
$\dot{E}_{Feed}$	feed exergy of the distillation column		
$OPEX_y$	Total annual operating expenses	**Greek symbols**	
		ω	acentric factor
		α	Modifying Function

1. Introduction

Gas condensate stabilization is the process of augmenting the intermediate and heavy compounds, i.e., $C_{3\text{-}5}$ and C_{6+}, within the gas condensate [1]. Thus, it can be stated that this process is an effort to eliminate light hydrocarbons, e.g., methane and ethane, from heavier hydrocarbons [2]. The principal aim of the process is to mitigate the pressure of vapor of condensate liquids to avoid the generated vapor phase upon flashing the liquid to atmospheric storage tanks [3]. Since the stabilized liquid possesses a vapor pressure, this stream is delivered to a pimping network or is sent into pressure vessels leading to an experience of the limitation of the pressure [4]. Moreover, concerning an appropriate gas condensate aimed at end-use frameworks, it is essential to take away components like free water, glycol, acidic contents, and salts [5].

According to the study by Campbell [6], two different methods of gas condensate stabilization were introduced. These methods include fractionation and multi-stage flash vaporization. The former (fractionation) is the most attractive technique dealing with removing the light fractions from the condensate gas by which the finalized product is made of heavy hydrocarbons and pentanes. Consequently, the product leaving the bottom side is a liquefied stream capable of storing at atmospheric pressure safely [7]. The second technique (flash vaporization) is based on the density difference between the vapor phase and liquid phase. Here, the vapor phase is steadily reduced up to the pressure of the liquified streams throughout each stage. Considering the equilibrium state between both phases, they reached the pressure and temperature of the separation [8].

Considering non-refluxed fractionation and multi-stage flash vaporization, Moghadam et al. [9] endeavored to stabilize gas condensate by diminishing its Reid Vapor Pressure (RVP) up to 10 psia. They considered two real gas refinery plants and stated that the use of each technique is associated with the operation of each plant. However, the first method is better than the second one. Tahouni et al. [10] utilized a reboiler and a two-stage compressor to increase the pheromone of a gas condensate stabilizer column. They stated that employing an extra heat transfer area of 1554 m² was able to enhance the productivity of the power by 20% and constantly maintain the consumed power. Salimi and Zarei [11] suggested and investigated the heat integration method to augment the ability of a gas condensate stabilization unit in Iran. This method led to saving 2.5 MW of power and decreasing the cost of the operation. Rahmanian et al. [12] parametrically analyzed the feasibility of a gas condensate stabilization unit and viewed the effect of the reboiler operating temperature, pressure, temperature, and flow rate of the feed on the sulfur content on the RVP. It was deduced that the dominant parameter was the reboiler operating temperature. In a study by Uwitonze et al. [13], the approach of stripping and heat integration was suggested to improve the possibility of a gas condensate stabilization unit. They indicated that for the controllability of the modification process, within a limited range of temperature, the process control performs properly. In order to enhance the productivity of the natural gas liquids (NGL) and liquefied petroleum gas (LPG), Bahmani et al. [14] proposed a modification process of a gas condensate stabilization unit aimed at reducing carbon dioxide (CO_2) emission. Hence, the productivity experienced about 4% enhancement leading to saving 360000$ annually and reducing 81 tons of CO_2. Hajizadeh et al. [15] optimized and parametrically analyzed a gas condensate stabilization unit leading to decreasing the required input energy by 20% at the optimum state. Furthermore, they indicated that the increase in the input flow rate of the feed upsurges the heat duty of each air cooler and splitter. In contrast, the reduction in the reflux ratio declined the heat duty of each splitter. Tavan et al. [16] simulated the process of condensate stabilization with a water draw pan. They studied the impact of input parameters, e.g., reboiler operating temperature and flow rate of excess water, on the

RVP and other variables. They also showed that the column with a water draw pan was more effective from the exergetic point of view in comparison with the column without a water draw pan. Hajizadeh et al. [17] tried to optimize the process of a gas condensate stabilization unit using the exergy approach. They could reduce the input power by 18% resulting in decreasing CO2 emissions up to 128 ton/day.

Attributable to the importance of the topic based on the literature survey and a few relevant studies, this study is motivated to perform a comparative study to modify the structure and optimize the operation of a gas condensate stabilization using five different arrangements:

* A stabilizer column with reboiler and condenser and without preheating (STB-A)

* A stabilizer column with reboiler and without condenser (STB-B)

* A stabilizer column with reboiler, without condenser and with preheating (STB-C)

* A stabilizer column with reboiler, condenser and preheater (STB-D)

* A stabilizer column with reboiler, without condenser and with side reboiler (STB-E)

This study is simulated using Aspen HYSYS software and Peng-Robinson fluid package. Furthermore, a comprehensive examination based on thermodynamic, cost, and environmental points of view along with sensitivity analysis is implemented.

The rest of this paper can be categorized as follows. In section 2, we describe the proposed model. In Section 3, the Simulation and methodology are discussed. In section 4 the results of the simulation are presented. Sections 5 and 6 analyze structures and sensitivity, respectively. The conclusion is also stated in section 7.

2. Model description

2.1.Structures of gas condensate stabilizer column

In this study, five structures are proposed for the stabilizer column, schematics of which are illustrated in Fig. 1. The objective of gas condensate stabilization is to remove the water and acid gases and reduce the Reid Vapor Pressure (RVP) of gas condensate. These structures have different thermodynamics and technical performances for the same feed (composition and operating conditions). In this paper, these different performances are analyzed and compared considering different aspects. In the following, the presented structures are described. The composition and operating conditions of the feed are given in Table 1.

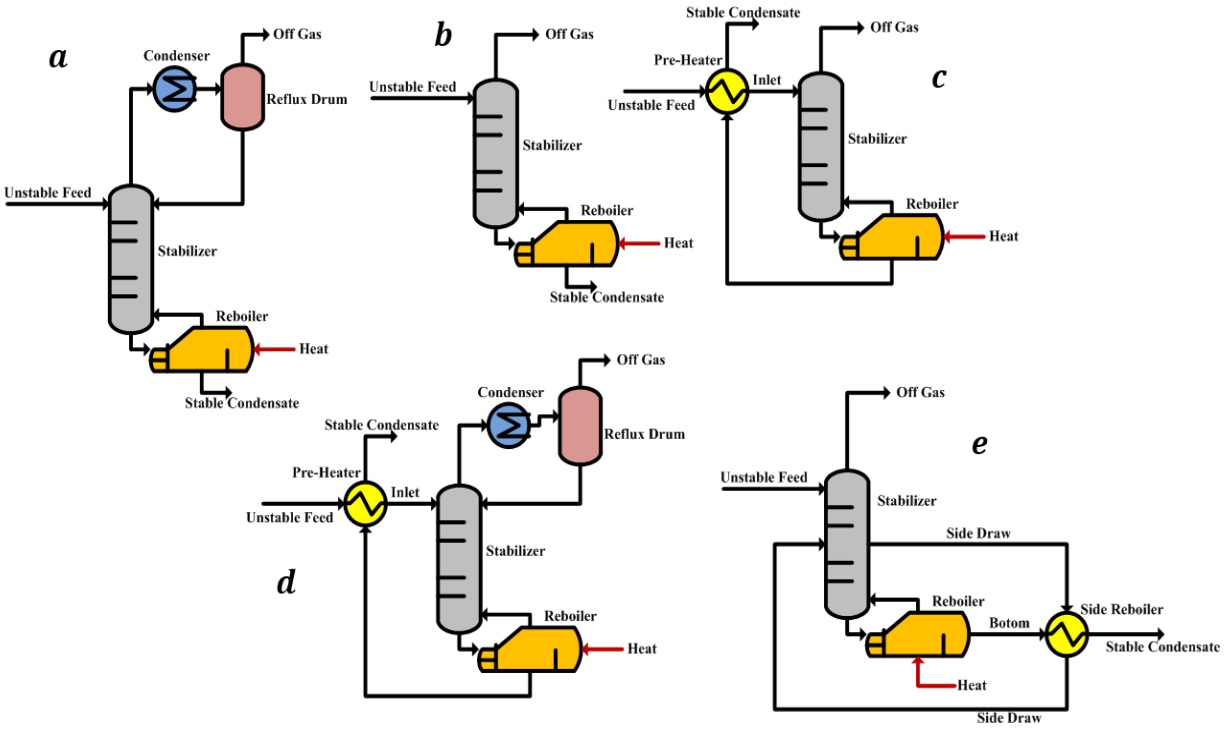

Fig. 1. Structures of gas condensate stabilizer column: a) stabilizer with reboiler and condenser, b) stabilizer with reboiler and without condenser, c) stabilizer with reboiler, without condenser and with preheater, d) stabilizer with reboiler, condenser, and preheater, e) stabilizer with reboiler without condenser, having a side reboiler.

Table 1. Specification of studied DGs.

Component	Mole fraction
water	۰.0005
Hydrogen sulfide	۰.0392
Carbon dioxide	۰.0125
Methane	۰.0609
Ethane	۰.0408
Propane	۰.0571
i-butane	۰.0273
n-butane	۰.058
i-pentane	۰.0445
n-pentane	۰.0472
hexane	۰.1053
heptane	۰.1299
octane	۰.1296
nonane	۰.0869
decane	۰.0588
n-C_{11}	۰.0341
n-C_{12}	۰.053
Methyl mercaptan	۰.009
Ethyl mercaptan	۰.0005
Dimethyl sulfide	۰.005
Operating conditions [16]	
Temperature (^{o}C)	23.1
Pressure (kPa)	934
Flow rate (kmol/h)	203.9

2.2. Stabilizer with reboiler and condenser (STB-A)

In this structure, unstable gas condensate with a vapor pressure (RVP) of 597.5 kPa (86.66 psia) from the first top tray enters the stabilizer column, where the reflux is supplied by the condenser, and from the top of the reflux drum the stabilized gas product exits. Reboiler of the stabilizer column removes the light component via vapor generation. Therefore, the stabilized condensate in this structure leaves in the liquid phase through the reboiler, while the vapor pressure of the gas condensate is reduced to 8 psia (Fig. 1a).

2.3. Stabilizer with reboiler and without condenser (STB-B)

This structure, shown in Fig. 1b, is a common method for the gas condensate stabilization process. In this structure, the stabilizer column is without the condenser, and the desorption process is carried out by the generated vapor in the reboiler. Unstable feed enters the column through the first tray. The low temperature of feed in the first tray of this structure causes the vapors to cool down. Stabilized condensate is produced in the reboiler of the stabilizer column.

2.4. Stabilizer with reboiler and preheater and without condenser (STB-C)

This structure is depicted in Fig. 1c. In this structure, thermal energy of the outlet product of the stabilizer's reboiler is employed to increase the feed temperature. Feed enters the column from the first top tray and there is no condenser. This structure uses thermal integration to reduce energy consumption. Off gas temperature in this structure is higher than those of thetwo previous structures since there is no condenser, and feed is injected from the top of the column at a higher temperature. The preheater is used for heat transfer between hot and cold streams. As a result, the stabilized condensate with a vapor pressure of 8 psia and at a lower temperature is produced in the preheater.

2.5. Stabilizer with reboiler, condenser, and preheater (STB-D)

This structure promotes the STB-C structure by adding a condenser and improves the STB-A structure (Fig. 1d) from the thermal integration aspect. Here, in addition to the condenser and reboiler, the stabilizer has a preheater for preheating the feed, which decreases the energy demand in the reboiler. In this structure, hot overhead

vapors of the stabilizer column enter the condenser. Due to the condensation part of the hydrocarbons are recovered at top of the column and are recirculated to the column. Similar to STB-C, the stabilized gas condensate is produced in the preheater at a lower temperature and with a reduced vapor pressure (8 psia).

2.6. Stabilizer with reboiler and side reboiler, without condenser (STB-E)

A Schematic of this structure is shown in Fig. 1e. This structure, which utilizes thermal integration via side reboiler method, tries to optimize the reboiler of the gas condensate stabilizer. Side reboiler in contrast to the preheater, mainly focuses on the stream that is drawn from the middle of column and enters the side reboiler at a low temperature to be preheated, and having higher temperature and energy content is re-fed to the same tray of the column. In this scenario, since the feed at low temperature enters the top tray there is no need for a condenser. This is because the low temperature of the feed at the top tray plays the role of a condenser. In this structure, heat of product of the reboiler is utilized to preheat the side stream and therefore the stabilized gas condensate is produced from the side reboiler at a temperature lower than the reboiler operating temperature and with a vapor pressure of 8 psia.

3. Simulation and methodology

Steady state simulation of mass and energy balance is the core part of computer-aided design. Process simulation allows an investigation of different process alternatives when feasibility studies are not possible. The main reasons for computer-aided simulations are [18]:

- Results of calculations in the design stage are necessary for the next steps.
- Designing to meet economic and operational limitations
- Using simulation, one can manage a large amount of produced information and apply it to improve and develop the desired process.

In this simulation study, Aspen HYSYS V10 is used to develop the models for the processes shown in Fig. 1 (Fig. 2). This software is a process simulator, which is extensively used in industries, especially for conceptual design and detailed engineering design and process monitoring, control and optimization of a project. The most important applications of Aspen HYSYS are in oil and gas treatment, refineries, and some air separation industries [19].

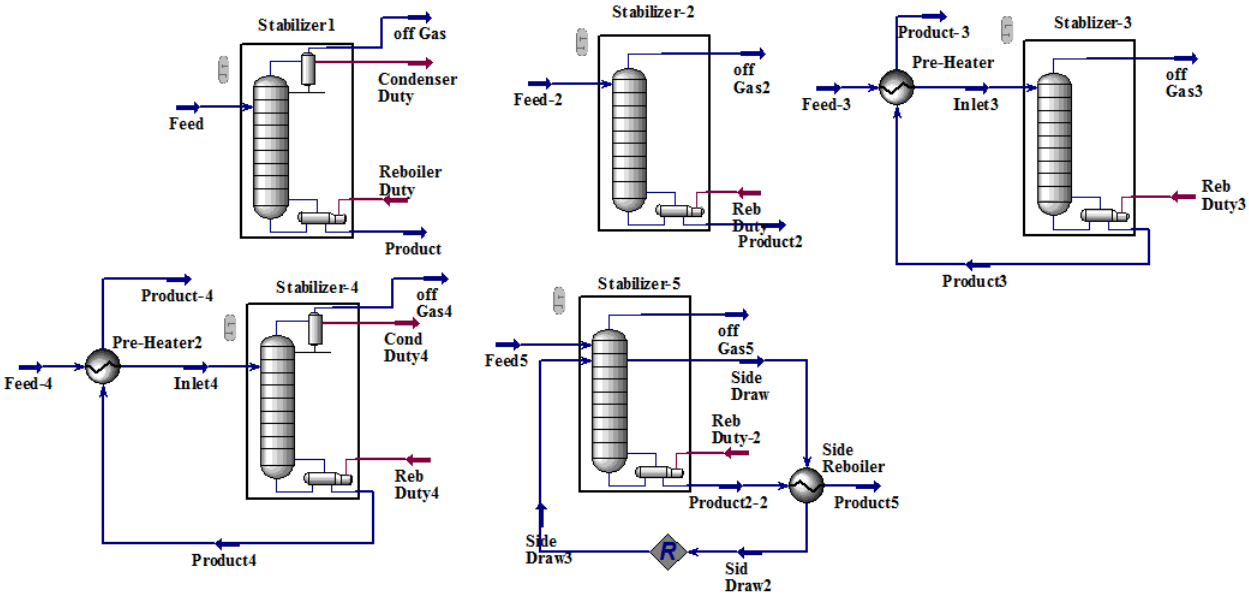

Fig. 2. Simulation schematics for the proposed structures of the gas condensate stabilizer column.

3.1.Fluid package

In Aspen HYSYS, thermodynamic equations are categorized as equations of state, activity equations, vapor pressure equations, and other equations (like acid gas property package). In this study, a fluid package should be selected that is suitable for the gas condensate stabilization process. In Table 2, the published papers on the natural gas treatment processes are listed. It can be said that researchers often have recommended using equations of state, among which the Peng-Robinson fluid package is better for simulation. Therefore, in the present paper, this equation of state is employed for simulating the structures proposed in Fig. 1.

Table 2. Previous studies on the hydrocarbon separation columns with the recommended equations of state.

Reference	Process	Equation of state
Zhu et al. [3]	gas condensate treatment	Peng Robinson
Moghadam et al. [9]	Gas Condensate Stabilization	Peng Robinson
Tahouni et al. [10]	condensate stabilization	Peng Robinson
Rahmanian et al. [12]	condensate stabilization	SRK
Uwitonze et al. [13]	Gas condensate stabilization	Peng Robinson
Saadi et al. [20]	LPG[2] Production	SRK[3]
Ching et al. [21]	Natural Gas Liquid (NGL) Fractionation	Peng Robinson
Junior et al. [22]	NGL recovery	Peng Robinson
Al-Ali [23]	crude oil stabilization	Peng Robinson
Yuan et al [24]	Natural Gas Liquefaction	Peng Robinson
Jung et al. [25]	Fractionation of NGL	Peng Robinson
Tamuzi et al. [26]	NGL fractionation	Peng Robinson
El-Eishy et al. [27]	Condensate Stabilization	Peng Robinson

Peng-Robinson equation of state first was developed in 1976 to accomplish the following goals [19]:

- This equation should be accurate to apply for calculating all properties of fluids in the natural gas processes (i.e., it should cover a wide range of gas processes).
- This model should be reasonable in particular for the compressibility factor and density of liquid near the critical point.
- Parameters should be extrapolated with respect to the acentric factor and critical properties.

Generally, Peng-Robinson equation of state produces results similar to Soave equation, while it gives more accurate predictions of density for most compounds in the liquid phase and specifically for nonpolar components [19]. The general form of the Peng-Robinson equation of state, which is mentioned recently, follows [20]–[27]:

$$P = \frac{RT}{V_m - b} - \frac{a\alpha}{V_m^2 + 2abV_m - b^2} \quad (1)$$

$$a = \frac{0.45724\, R^2 T_c^2}{P_c} \quad (2)$$

$$b = \frac{0.07780\, RT_c}{P_c} \quad (3)$$

$$\alpha = \left\{1 + (0.37464 + 1.5422\omega - 0.26992\omega^2)\left(1 - T_r^{0.5}\right)\right\}^2 \quad (4)$$

where a and b are the equation constants that depend on the critical temperature and pressure (2), (3). In addition, modifying function α depends on temperature and acentric factor (ω) (4).

The benefits of using this property package in Aspen HYSYS are as follows [28]:

- High accuracy at wide ranges of temperature and pressure
- Special treatment for key components
- Extensive data bank for binary parameters
-

3.2. Stabilizer column specifications and simulation assumptions

The stabilizer column of this study for stabilizing the gas condensate is located in Ilam Gas Treating Company (IGTC) in Iran [29]. Based on IGTC operating documents, the stabilizer possesses 15 trays, from the first top of which the feed (Table 1 [16]) is fed. Pressures at the top and bottom of the stabilizer column are 1001 and 1014 kPa [29]. In this paper, to simulate the structures proposed in Fig. 1, the following assumptions are considered:

- The number of trays for all the structures are equal.
- Operating conditions and composition of the feed are identical.
- Operating pressures at the top and bottom of the stabilizer are similar in all the configurations.
- The maximum temperature for preheating the condensate to enter the stabilizer is 90 °C.
- The simulated system is in steady state.
- Heat losses in the heat exchangers are negligible.
- The temperatures of the condenser in all structures that use one are identical and equal to 35 °C.
- In all structures, the column is simulated in a way that the RVP of gas condensate equals 8 psia.
- Pressure drops in the preheater and side reboiler are zero.

[2] - Liquefied Petroleum Gas
3 - Soave-Redlich-Kong

4. Results of the simulation

To simulate the proposed structures, it is required to apply the basic data and assumptions in the flowsheet. This information was given in the previous sections and using the appropriate equation of state all the thermodynamic properties are obtained at all process points. Based on the equation of state calculations the results of mass and energy are obtained, and the results of the structures simulations are given in Tables 3 to 5.

Table 3. Operating conditions at the process points (names of streams are according to Fig. 2)

Streams	P (kPa)	T (℃)	Flow ($\frac{kmole}{h}$)	Streams	T (℃)	P (kPa)	Flow ($\frac{kmole}{h}$)
Feed	934	23.1	203.9	off Gas	35	1001	49.37
Product	1014	179.1	154.5	off Gas2	47.55	1001	49.57
Product2	1014	179.1	154.3	Inlet3	90	934	203.9
Product-3	1014	111.2	147.1	Product3	182	1014	147.1
off Gas3	1001	92.93	56.78	off Gas5	47.78	1001	49.62
Product2-2	1014	179.1	154.3	Product5	123.4	1014	154.3
Side Draw	1008	119.8	200	Sid Draw2	148	1008	200
off Gas4	1001	35	50.59	Product4	179.9	1014	153.3
Inlet4	934	90	203.9	Product-4	111.3	1014	153.3

Table 4. Mass balance (mole fraction) for the products of the gas condensate stabilizer structures.

	STB-A		STB-B		STB-C		STB-D		STB-E	
	Off gas	Condensate	Off gas	Condensate	Off gas	Condensate	Off gas	Condensate	Off gas	Condensate
Water	0.00	0.00	0.00	0.00	0.00	0.00	0.00	0.00	0.00	0.00
H_2S	0.16	0.00	0.16	0.00	0.14	0.00	0.16	0.00	0.16	0.00
CO_2	0.05	0.00	0.05	0.00	0.04	0.00	0.05	0.00	0.05	0.00
Methane	0.25	0.00	0.25	0.00	0.22	0.00	0.25	0.00	0.25	0.00
Ethane	0.17	0.00	0.17	0.00	0.15	0.00	0.16	0.00	0.17	0.00
Propane	0.24	0.00	0.23	0.00	0.19	0.00	0.23	0.00	0.23	0.00
i-Butane	0.04	0.02	0.04	0.02	0.04	0.02	0.04	0.02	0.04	0.02
n-Butane	0.04	0.06	0.04	0.06	0.07	0.05	0.06	0.06	0.04	0.06
i-Pentane	0.01	0.06	0.01	0.06	0.03	0.05	0.02	0.05	0.01	0.06
n-Pentane	0.01	0.06	0.01	0.06	0.03	0.05	0.01	0.06	0.01	0.06
n-Hexane	0.01	0.14	0.01	0.14	0.03	0.13	0.01	0.14	0.01	0.14
n-Heptane	0.00	0.17	0.00	0.17	0.02	0.17	0.00	0.17	0.00	0.17
n-Octane	0.00	0.17	0.00	0.17	0.01	0.18	0.00	0.17	0.00	0.17
n-Nonane	0.00	0.11	0.00	0.11	0.00	0.12	0.00	0.12	0.00	0.11
n-Decane	0.00	0.08	0.00	0.08	0.00	0.08	0.00	0.08	0.00	0.08
c-C11	0.00	0.04	0.00	0.05	0.00	0.05	0.00	0.05	0.00	0.05
n-C12	0.00	0.07	0.00	0.07	0.00	0.07	0.00	0.07	0.00	0.07
CH_3SH	0.03	0.00	0.03	0.00	0.02	0.01	0.02	0.01	0.02	0.00
C_2H_5SH	0.00	0.00	0.00	0.00	0.00	0.00	0.00	0.00	0.00	0.00
diM-Sulfide	0.00	0.01	0.00	0.01	0.00	0.01	0.00	0.01	0.00	0.01

Table 5. Energy balance for the proposed structures.

	STB-A	STB-B	STB-C	STB-D	STB-E
Reboiler Duty($\frac{GJ}{h}$)	7.074	7.063	7.264	4.472	4.483
Condenser Duty($\frac{GJ}{h}$)	0.0483	-	-	0.5419	-
Preheater Heat Exchange($\frac{GJ}{h}$)	-	-	3.123	3.123	-
Side Reboiler Heat Exchanged ($\frac{GJ}{h}$)	-	-	-	-	2.582

5. Analysis of the structures

5.1. Energy and utility analysis

In this study, one of the objectives of proposing the structures for gas condensate stabilizer is to achieve a structure with optimum thermodynamic performance. In the first structure (STB-A), the unstable gas condensate stream is injected into the distillation column without any preheating and then stabilization is performed. According to the simulation results, in this case, energy consumption of the reboiler is 1965 kW, which corresponds to steam consumption equal to 3075 $\frac{kg}{h}$ at operating conditions of 165 psia (saturated vapor).

For the stabilizer condenser in structure STB-A, according to the results of Aspen Energy Analyzer the consumption of cooling water is 275 Gallons per hour, which is employed to achieve a condensation temperature of 35 ^{o}C. In structure STB-B, the stabilizer has a reboiler and no condenser. Here, the feed is not preheated and is injected directly into the stabilizer column. Thus, all the utility consumption is in the reboiler.

Based on the simulation results, reboiler energy in this structure is 1962 kW and is equal to consumption of 3071 $\frac{kg}{h}$ steam at operating condition of 165 psia (saturated vapor). Since there is no condenser and reflux stream, it is observed that hot utility consumption in the scenario STB-B is lower than that in structure STB-A. Nevertheless, accounting for cold utility consumption in the condenser, total utility consumptions in scenarios STB-A and STB-B are 1978.42 kW and 1962 kW, respectively.

In structure STB-C, conditions are changed and a part of reboiler energy is compensated by the preheating of the raw condensate feed. According to the simulation results, in preheater, the heat transfer rate between hot stream (182 ^{o}C) and cold stream (^{o}C) is 867.6 kW. At such conditions, energy consumption in the reboiler of stabilizer is 1179 kW, which is equivalent to hot utility consumption of 1846.46 $\frac{kg}{h}$ of steam (at the operating condition of 165 psia). Since there is no condenser in this structure, cold utility consumption is zero and in structure STB-C, total utility consumption is estimated as 1179 kW, which compared to structures STB-A and STB-B shows a 40.41% and 39.91% decrease, respectively. As a result, it can be said that the STB-C is more optimized compared to STB-A and STB-B since it saves 10012.6 and 9980 $\frac{kg}{year}$ steam (hot utility) in comparison to STB-A and STB-B, respectively.

Structure STB-D tries to optimize the structure STB-A by using the preheater, and for this purpose, temperature of the inlet feed to the stabilizer increases to 90 ^{o}C using the hot outlet stream of the stabilizer reboiler. According to the simulation, the heat transfer rate in this heat exchanger is 867.6 kW, which this amount of recovered heat results in a 1242 kW of energy consumption in the reboiler of stabilizer (1945 $\frac{kg}{h}$ steam at 165 psia), which in comparison to scenario STB-A shows a 36.79% decrement. Due to the existence of a condenser in this scenario, cold utility is also consumed which is equal to 3081 gallons per hour for cooling down the temperature of overhead vapors of the column to 35 ^{o}C. Total utility consumption in structure STB-D is 1392.5 kW, which is lower than that of structure STB-A by 29.62%.

In addition, according to the performed analysis, structure STB-D is more optimized than the structure STB-B and its total utility consumption is 29% lower. However, conditions are different in comparison with structure STB-C and the lack of condenser leads to a 15.3% decrease in total utility consumption in structure STB-C compared to STB-D. As a result, for gas condensate stabilization, STB-C has lower utility consumption in comparison to STB-A, STB-B, and STB-D.

Structure STB-E is the improved version of structure STB-B and for improvement, the side reboiler technique is utilized. The side reboiler has a similar function as the preheater. The side reboiler in structure STB-E increases the temperature of side stream, with a flow rate of 200 $\frac{kmole}{h}$, from 119.8 ^{o}C up to 148 ^{o}C. The heated stream is recirculated to the stabilizer with higher energy content and therefore with a heat transfer rate of 717.2 kW reduces energy consumption of the reboiler to 1245 kW (1948.82 $\frac{kg}{h}$ steam at 165 psia). While in the stabilizer column, to cool down vapors produced in stabilization the low temperature of the inlet feed (23.1 ^{o}C) is utilized instead of a condenser, and cold utility consumption is saved.

According to Fig. 3, structure STB-C has lower total utility consumption than other structures. Based on the performed analysis, total utility consumption in structure STB-C in comparison to the structures STB-A, STB-B, STB-D, and STB-E is lower by 40.39%, 39.91%, 15.33%, and 5.3%, respectively. Thus, it can be said that structure STB-C stabilizes the condensate with lower utility consumption.

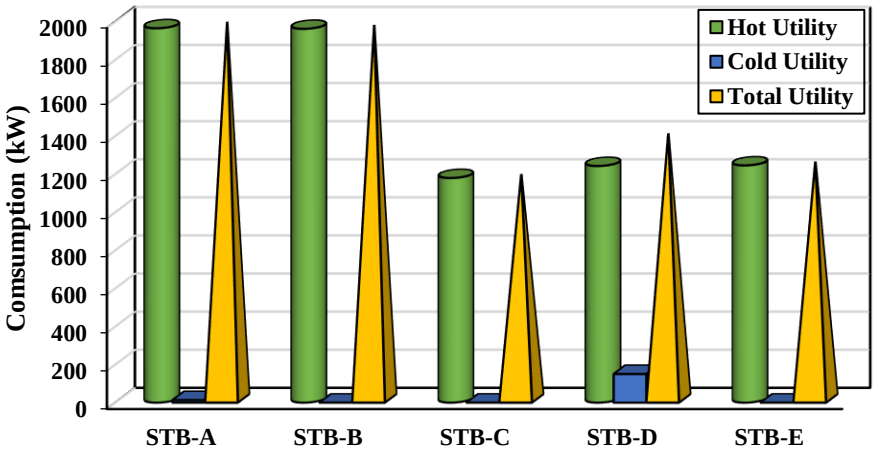

Fig. 3. Comparison between utility consumption in the proposed structures for stabilizer column.

5.2. Vapor to feed ratio

In the gas condensate stabilization process, always some of the hydrocarbons lost through the stabilized vapors. To avoid the loss either a condenser is employed (structures STB-A and STB-D), or the raw condensate stream with a low temperature is injected into the column from the first top tray to the stabilized column like in structures STB-B, STB-C, and STB-E. Therefore, decreasing this hydrocarbon loss through the overhead vapors of the column ($\dot{G}_{vapor}$) is important and it should be minimized. Thus, in this paper a parameter called vapor to feed ratio (VTF ratio) is defined (5):

$$VTF = \left(\frac{\dot{G}_{vapor}}{\dot{G}_{Feed}}\right)_{mole\ basis} \quad (5)$$

Lower this parameter is, a smaller portion of the inlet feed ($\dot{G}_{Feed}$) is lost through the vapor. In other words, the gas condensate stabilization process should be performed so other hydrocarbons loss be prevented while the quality of RVP is maintained. For this reason, during the simulation of structures RVP of the gas condensate product is considered fixed at 8 psia. According to Fig. 4, structure STB-C has the largest VTF ratio, which represents the maximum hydrocarbon loss through overhead vapors of the stabilizer in this scenario. In structure STB-C, raw condensate feed after reaching the temperature of 90 °C, enters the column from the top tray, and because there is no condenser in this structure a large portion of the hydrocarbons (28%) is lost directly through overhead vapors of the column. However, in structure STB-E, the VTF ratio reaches its minimum and the hydrocarbon loss decreases in comparison to structures STB-C and STB-D by 16.67% and 4.17%, respectively. Other structures because of using a condenser and/or injection of feed from the first top tray perform better than structures STB-D and STB-C; however, quantitatively structure STB-E results in the lowest value for the VTF ratio.

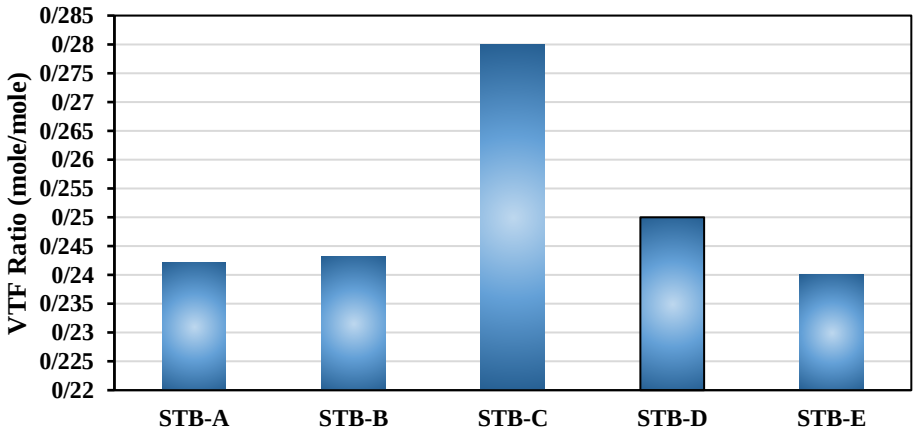

Fig. 4. Comparison between values of VTF ratio of the structures.

5.3. Exergy analysis

In the present study, the main objective of the exergy analysis is to calculate the exergy destruction and exergy efficiency of the gas condensate stabilizer column in the structures shown in Fig. 1. Exergy efficiency of the stabilizer column can be determined by (6) [30]:

$$\eta_{exergy}^{STB} = \frac{W_{min}}{W_{min} + \dot{E}_D^{STB}} \quad (6)$$

in (6), W_{min} is the minimum work for the separation, which can be calculated by (7) [30]:

$$W_{min}(kW) = \sum \dot{E}_{products} - \dot{E}_{Feed} \quad (7)$$

In addition, $\dot{E}_D^{STB}$ is the total exergy destruction of the stabilizer column, and (8) should be employed for its calculation [30]:

$$\dot{E}_D^{STB} = \dot{E}_{Feed} - \sum \dot{E}_{products} + \dot{Q}_R\left(1 - \left(\frac{T_0}{T_R}\right)\right) - \dot{Q}_C\left(1 - \left(\frac{T_0}{T_C}\right)\right) \quad (8)$$

in (8), $\dot{E}_{Feed}$ is the feed exergy of the distillation column, $\dot{E}_{products}$ is the exergy of condensate products and residues of the stabilizer, $\dot{Q}_R$ is the net duty of reboiler, $\dot{Q}_C$ is the net duty of condenser, T_0 is the ambient temperature, T_R is the temperature of reboiler, and T_C is the temperature of the condenser.

Since the stabilization process is a physical separation process the total exergy of each stream only consists of the physical exergy. Physical exergy can be obtained from (9), where H is the enthalpy and S is the entropy of stream i [30].

$$\dot{E}_i^{PH} = H - T_0 S \quad (9)$$

Based on the operating information of the process streams that are listed in Table 3 and using the property module of Aspen HYSYS, enthalpy and entropy of process points are obtained, which are used to calculate the physical exergy of the streams, values of which are given in Table 6. Then, based on (7) and (8) the related parameters are calculated, and results for each proposed structure are reported separately in Table 7.

Table 6. Physical exergy of process streams for stabilizer structures.

Stream	$\dot{E}_i^{PH}$(kW)	Stream	$\dot{E}_i^{PH}$(kW)
Feed	56.2	off Gas	75.15
Feed2	56.2	Product	370.2
Feed3	56.2	off Gas2	75.95
Feed4	56.2	Product2	370.2
Feed5	56.2	off Gas3	93.15
Inlet3	139.7	Product3	368.8
Inlet4	139.7	Product4	371.6
off Gas4	76.84	Product2-2	369.9
off Gas5	76.04		

Table 7. Results of exergy calculations of stabilizer columns based on the proposed structures.

STB-A	
$\dot{Q}_R\left(1 - \left(\frac{T_0}{T_R}\right)\right)$	1688
$\dot{Q}_C\left(1 - \left(\frac{T_0}{T_C}\right)\right)$	3.835
W_{min}	389.2
$\dot{E}_D^{STB}$(kW)	1295
η_{exergy}^{STB}	0.2311

STB-B	
$\dot{Q}_R\left(1-\left(\frac{T_0}{T_R}\right)\right)$	1688
$\dot{Q}_C\left(1-\left(\frac{T_0}{T_C}\right)\right)$	0
W_{min}	390
$\dot{E}_D^{STB}$(kW)	1298
η_{exergy}^{STB}	0.231
STB-C	
$\dot{Q}_R\left(1-\left(\frac{T_0}{T_R}\right)\right)$	1017
$\dot{Q}_C\left(1-\left(\frac{T_0}{T_C}\right)\right)$	0
W_{min}	322.3
$\dot{E}_D^{STB}$(kW)	694.5
η_{exergy}^{STB}	0.317
STB-D	
$\dot{Q}_R\left(1-\left(\frac{T_0}{T_R}\right)\right)$	1070
$\dot{Q}_C\left(1-\left(\frac{T_0}{T_C}\right)\right)$	43.01
W_{min}	308.7
$\dot{E}_D^{STB}$(kW)	717.8
η_{exergy}^{STB}	0.3007
STB-E	
$\dot{Q}_R\left(1-\left(\frac{T_0}{T_R}\right)\right)$	1072
$\dot{Q}_C\left(1-\left(\frac{T_0}{T_C}\right)\right)$	0
W_{min}	389.7
$\dot{E}_D^{STB}$(kW)	681.9
η_{exergy}^{STB}	0.3637

According to Fig. 5, exergy destruction of structure STB-E is lower than of the other structures. Based on (7) and (8) it can be said that the lower value for VTF ratio along with employing side reboiler are the two factors that in structure STB-E first decreases the exergy destruction and second increases the exergy efficiency of the stabilizer column. Based on Fig. 7 and 8, it can be deduced that exergy destruction is directly related to the exergy efficiency of the distillation column. According to the performed analysis, exergy destruction of structure STB-E in comparison to those of structures STB-A, STB-B, STB-C, and STB-D is lower by 47.34%, 47.47%, 1.81%, and 5%, respectively. Therefore, as it is shown in Fig. 6, this decrease in exergy destruction positively affects the exergy efficiency of the

stabilizer column. In general, structure STB-E possesses the highest thermodynamic efficiency.

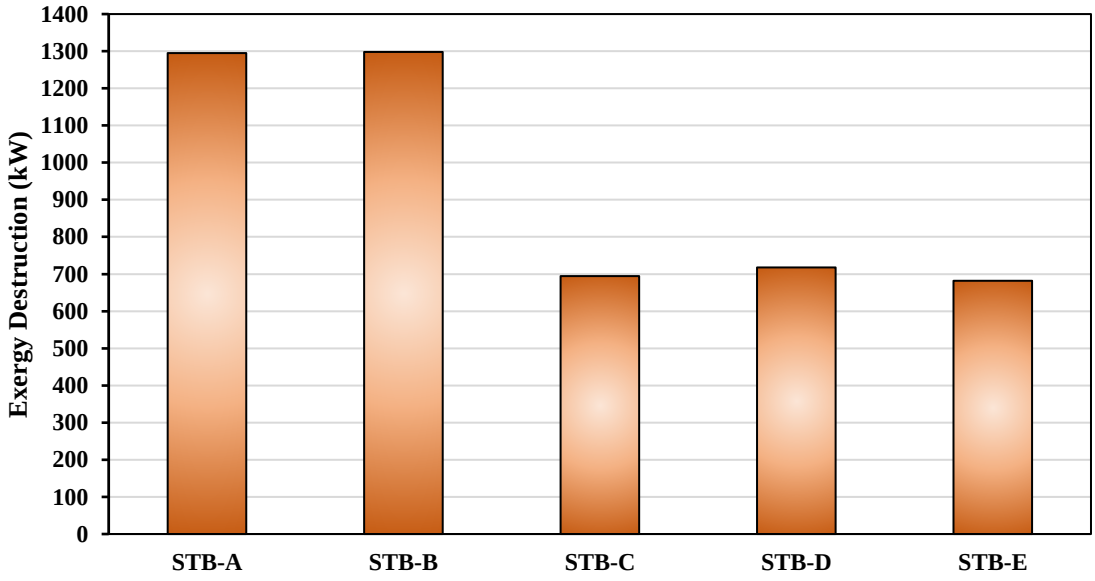

Fig. 5. Comparison between exergy destruction of different structures of the stabilizer columns

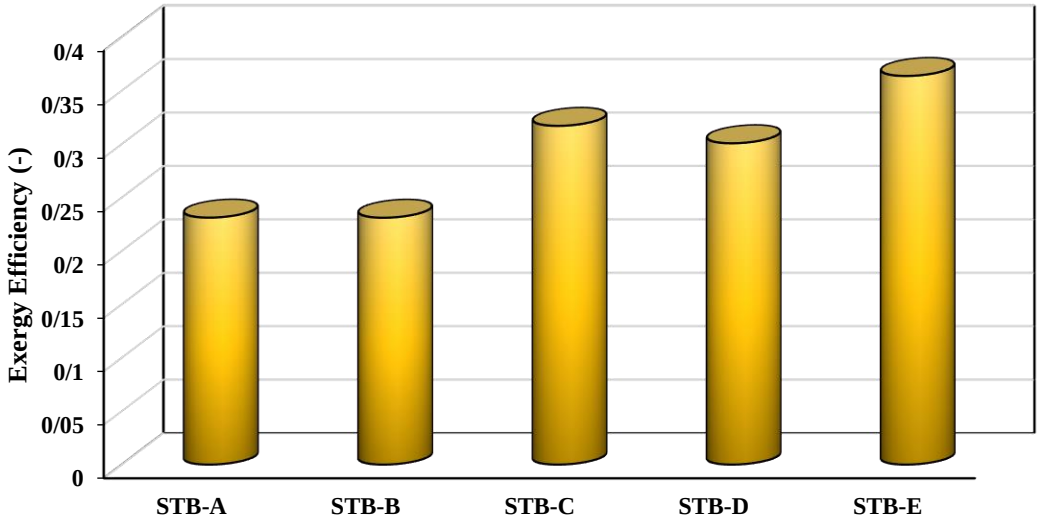

Fig. 6. Comparison between the exergy efficiency of the stabilizer column in the proposed structures

5.4. CO2 emission analysis

Carbon dioxide emits in three ways: through the process streams, which is called direct emission, and through heat and electricity consumption, which in total form the indirect emissions. Therefore, the total CO_2 emission (10) by the base and proposed processes are the summation of direct and indirect emissions [30]:

$$CO_{2,emission}^{total} = CO_{2,emission}^{direct} + CO_{2,emission}^{indirect} \quad (10)$$

In the proposed structures, direct emission ($CO_{2,emission}^{direct}$) is only due to the overhead vapors of the stabilizer column, while indirect emission ($CO_{2,emission}^{indirect}$) is purely because of steam consumption in the reboiler. According to the performed analysis, to supply each MMBtu of heat in reboiler 205.3 pounds of CO_2 is produced [31]. From the simulation flowsheet, duty of reboiler in $\frac{MMBtu}{h}$ and indirect CO_2 emission in $\frac{kg}{h}$ can be calculated and reported. In Table 8, CO_2 emissions for the proposed structures are listed.

As a general conclusion, it should be said that based on Table 8 in all the structures the indirect emission contribution to the total emission ($CO^{total}_{2,emission}$) is much higher than the direct emission (on average between 74% to 83%). Structures STB-A and STB-B because do not employ energy optimization, have higher steam consumption, which eventually results in the highest emission. However, in structures that employ optimization, the emission is lower. This demonstrates the importance of energy optimization and its relationship with the environment more clearly.

Table 8. Parameters of CO2 emission for the proposed structures

Parameters	STB-A	STB-B	STB-C	STB-D	STB-E
$CO^{direct}_{2.emission}(\frac{kg}{h})$	112.16	112.16	112.16	112.16	112.16
$CO^{indirect}_{2.emission}(\frac{kg}{h})$	542	541	325	343	344
$CO^{total}_{2.emission}(\frac{kg}{h})$	654.16	653.16	437.16	455.16	456.16

5.5. Economic analysis

In this study, the main goal of the economic analysis is to predict the total annual cost (TAC) and total product cost (TPC) (11) and (15) [30]:

$$\text{total annual cost (TAC)} = CAPEX_y + \text{total operating cost From APEA} \quad (11)$$

Total annual operating expenses ($OPEX_y$) equals summation of variable operating cost (VOC) and Fixed operating cost (FOC) (12) [32]. In this study, Aspen Process Economic Analyzer (APEA) tool is used to calculate the annual operating expenses for all the structures in dollars per year. The variable operating cost includes the costs of energy (electricity and steam) and cooling water supply [32].

$$\text{total operating cost } (OPEX_y) = VOC + FOC \quad (12)$$

In addition, to calculate the annual capital expenditures ($CAPEX_y$), first, the capital expenditure CAPEX is determined by the APEA tool, then using the Capital Recovery Factor (CRF) it is converted to the annualized value (according to (13)) [32]:

$$CAPEX_y = CAPEX \text{ From APEA} \times \frac{i \times (1+i)^n}{(1+i)^n - 1} \quad (13)$$

In (13), it is assumed that the decreasing rate of the bank interest (i or discount rate) is 8.5%, and the economic lifetime of the project (n) is 30 years [32]. Therefore, based on what is said, (12) can be rewritten as (14).

$$TAC\ (\frac{USD}{year}) = CAPEX \times \frac{i \times (1+i)^n}{(1+i)^n - 1} + OPEX_y \quad (14)$$

In Table 9, the economic parameters for the proposed structures are reported. Here, in addition to the stabilizer column, in the economic calculations, the assembled equipment like the heat exchangers for the optimization are also considered. Based on the obtained results, structures STB-A and STB-B have the highest total annual cost (TAC). It is also demonstrated that the structure STB-C has the lowest TAC since there is no condenser in the stabilizer column and it also employs the optimization technique of feed preheating. It should be noted that in the structure STB-C, due to the high value of VTF ratio, some portion of valuable hydrocarbons like propane and butanes are lost which emphasizes the definition of the total product cost (TPC). Total product cost is calculated by (15), where $\dot{m}_{product}$ is the mass flow rate of the gas condensate in $\frac{kg}{year}$. Based on TPC definition it is revealed that in the structures that utilize optimization, the production cost for each kilogram of gas condensate is lower, and these structures are more justifiable from the economic point of view compared to the structures that do not employ optimization.

In other words, structures with optimization have total product costs lower than structures STB-A and STB-B by 7.14%. Therefore, economic results show that the using optimization methods like side reboiler and preheater in the process of gas condensate stabilization results in a lower value for the key and competitive parameter of TPC in comparison to the conventional methods.

$$\text{total product cost } \left(\frac{USD}{kg}\right) = \frac{TAC}{\dot{m}_{product}} \quad (15)$$

Table 9. Summary of calculation of economic parameters for the proposed structures (column plus heat exchangers).

Parameter	STB-A	STB-B	STB-C	STB-D	STB-E
CAPEX	2620570	2341240	2676010	2897420	2804870
$CAPEX_y$ $(\frac{USD}{year})$	243846	217854	249004	269607	260995
VOC $(\frac{USD}{year})$	704175	702859	450755	475585	473410
FOC $(\frac{USD}{year})$	984605	978961	961025	963185	966640
$OPEX_y$ $(\frac{USD}{year})$	1688780	1681820	1411780	1438770	1440050
TAC $(\frac{USD}{year})$	1932626	1899674	1660784	1708377	1701045
Total product cost $(\frac{USD}{kg})$	0.014	0.014	0.013	0.013	0.013

6. Sensitivity analysis

6.1. Effect of temperature in structures STB-C and STB-D

Studying the effect of stabiliser feed temperature on reboiler duty is shown in Fig. 7. According to Fig. 7, the reboiler's energy usage decreases as the feed temperature rises in structures STB-C and STB-D. The reboiler duty's downward tendency is more substantial in structure STB-C than it is in structure STB-D. This is due to the condenser and recirculating stream in structure STB-D, where more reflux liquid is recirculated to the stabiliser column as the feed temperature rises. The VTF of structure STB-C exhibits a climbing trend as the stabiliser feed temperature rises, as seen in Fig. 8. Because there is no condenser in the STB-D construction, the growing tendency is more noticeable. Due to the absence of a condenser in structure STB-C, the growing tendency is more notable in STB-D. In the STB-D construction, the condenser restrains the discharge of the vapours, and some of the stream is recovered in the liquid phase after cooling. As a result, in structure STB-C, raising the temperature of the stabiliser column feed causes hydrocarbon loss, resulting in a decreased flow rate of gas condensate under these circumstances.

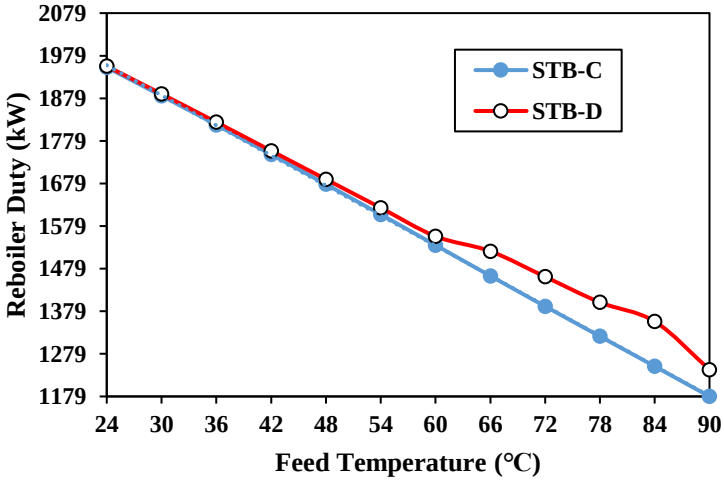

Fig. 7. Effect of the stabilizer feed temperature on the reboiler duty.

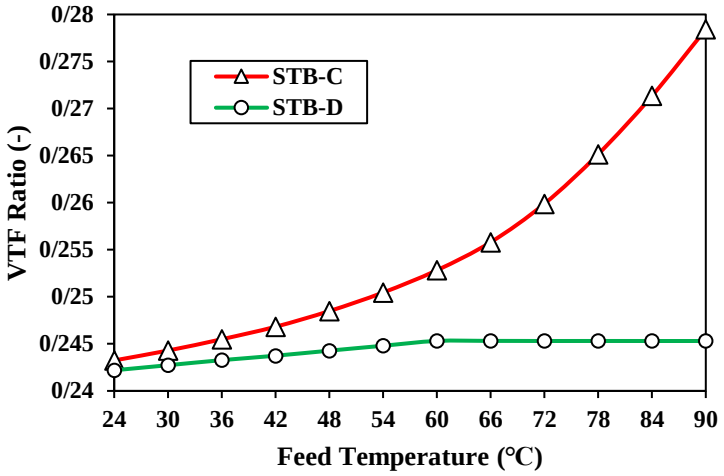

Fig. 8. Effect of stabilizer feed temperature on the vapor to feed ratio.

According to Fig. 9, the exergy efficiency of the column increases as the temperature of the stabilizer column feed is raised. Both STB-C and STB-D structures exhibit this finding; however, STB-C structure has a higher quantity of exergy efficiency.

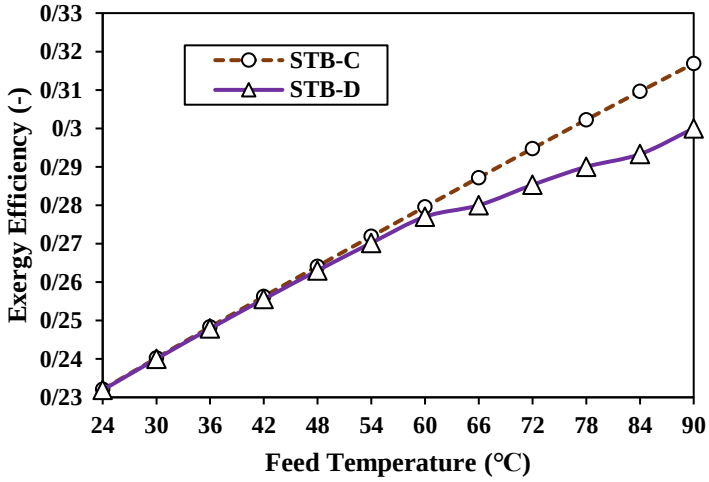

Fig. 9. Effect of stabilizer feed temperature on the exergy efficiency.

6.2. Effect of side draw rate in structure STB-E

According to Fig. 10, increasing the flow rate of the side stream, which acts as the working fluid of heat transfer in structure STB-E, decreases the reboiler duty and total exergy destruction of the stabilizer column. An increase in the side draw rate leads to increasing the heat transfer in the side reboiler, and this somehow causes the energy demand in the main reboiler of the stabilizer to decrease. Since the reboiler of the stabilizer column has the highest energy consumption, any decrease in its energy consumption leads to a decline in the total exergy destruction of the stabilizer column and consequently an increase in exergy efficiency, which is shown in Fig. 11.

Energy and environment are interdependent. Thus decreasing the utility consumption directly affects the direct and total CO_2 emission decrement. According to Fig. 12, when the side draw rate increases total CO_2 emission in the structure STB-E decreases. As was mentioned, in all structures the main contribution to the CO_2 emission is from the reboiler of the column. Based on Fig. 10, increasing the side draw rate decreases the reboiler duty, which means a decrease in utility consumption and consequently in indirect CO_2 emission.

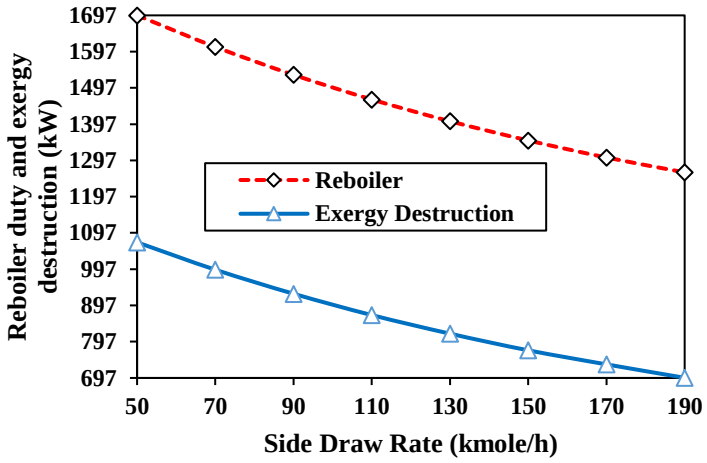

Fig. 10. Effect of side draw rate on the reboiler duty and exergy destruction of the stabilizer column.

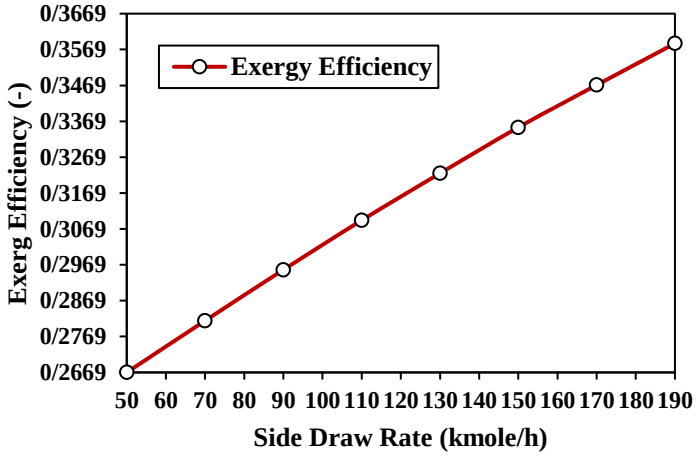

Fig. 11. Effect of side draw rate on the exergy efficiency of the stabilizer column.

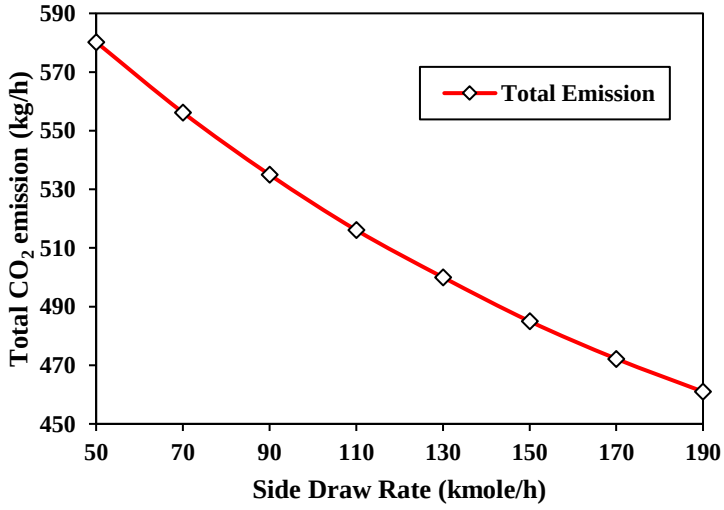

Fig. 12. Effect of side draw rate on total CO_2 emission.

7. Conclusion

Gas condensate or natural gasoline is a stream of hydrocarbons consisting of acid gases, water, oil cuts (specifically light and heavy naphtha), and light gases like methane to butane. This stream usually is in a two-phase state and its main portion is in the liquid phase. Due to the existence of valuable hydrocarbons like aromatics, and other cyclic compounds, this stream has high economic value in addition to its heating value. Currently, there are two methods to stabilize the gas condensate worldwide, the vapor-liquid equilibrium method and the distillation method, which the latter is more common.

In this paper, the focus was on the gas condensate stabilization with the distillation method in a column called stabilizer. For this purpose, five different structures of stabilizer are simulated and analyzed from technical, economic, and environmental points of view. According to the performed analysis, when the condensate stabilizer works without any thermal integration (without side reboiler and preheater) its exergy destruction, CO_2 emission, and reboiler duty are higher, and its exergy efficiency is lower. In addition, based on the economic analysis, not using optimization structures leads to an increase in the competitive parameter of total product cost. Technical analysis of the VTF ratio showed that if preheating of stabilizer inlet feed is utilized and if the column has no condenser, hydrocarbon loss through the stable vapors increases, and eventually flow rate of the gas condensate product decreases. In other words, although feed preheating leads to an increase in the exergy efficiency, decrease in reboiler energy consumption, and decrease in pollutants emission, if the stabilizer column has no reflux the production flow rate of gas condensate encounters serious challenges.

In addition, the economic analysis showed that in structures that use side reboiler and preheater techniques for optimization of the stabilizer column, total product cost is identical. However, when different parameters are compared for choosing the suitable option, structure STB-E is the most appropriate choice. Based on the performed evaluation, in this structure, all energy, exergy, economic and environmental aspects have suitable values and it has perfect specifications for gas condensate stabilization. In this structure, using the side reboiler leads to reboiler optimization and increasing of thermodynamic efficiency. On the other hand, due to entering the feed at the first top tray with low temperature, there is no need for a condenser, which leads to the lowest value for hydrocarbon loss. Finally, it can be said that gas condensate stabilization in a reboiler stabilizer with a side reboiler is a suitable structure since in addition to thermodynamic improvement in the stabilization process, it prevents the valuable hydrocarbon loss.

For future work, it is proposed to evaluate the energy, exergy, economic and environmental performance of a gas stabilization unit through a real-time optimization (RTO) strategy. A detailed sensitivity analysis is also performed using the response surface method to evaluate the relative importance of operational parameters on objective functions, such as exergy efficiency, energy cost, and CO2 emissions.

REFERENCES

[1] S. Mokhatab, W. A. Poe, and J. Mak, *Handbook of natural gas transmission and processing: principles and practices*. Gulf professional publishing, 2018.

[2] H. Adib, A. Sabet, A. Naderifar, M. Adib, and M. Ebrahimzadeh, “Evolving a prediction model based on machine learning approach for hydrogen sulfide removal from sour condensate of south pars natural gas processing plant,” *J Nat Gas Sci Eng*, vol. 27, pp. 74–81, 2015.

[3] L. Zhu, H. Liu, Z. Zhang, and Y. Pu, “Simulation analysis of stripping fractionation process of gas condensate treatment and practical application,” *J Nat Gas Sci Eng*, vol. 34, pp. 216–225, 2016.

[4] C. Zheng, Z. Liu, Q. Liu, Y. Li, and C. Liu, “Comparative investigation on corrosion behavior of laser cladding C22 coating, Hastelloy C22 alloy and Ti–6Al–4V alloy in simulated desulfurized flue gas condensates,” *Journal of Materials Research and Technology*, vol. 18, pp. 2194–2207, 2022.

[5] C. J. Geankoplis, “Separation Process Principles,” 2003.

[6] O. A. Boniface and E. Egoyibo, “Natural Gas Conditioning and Processing from Marginal Fields Using Modular Technology in Nigeria”.

[7] I. Vlastélic, T. Staudacher, P. Bachèlery, P. Télouk, D. Neuville, and M. Benbakkar, “Lithium isotope fractionation during magma degassing: constraints from silicic differentiates and natural gas condensates from Piton de la Fournaise volcano (Réunion Island),” *Chem Geol*, vol. 284, no. 1–2, pp. 26–34, 2011.

[8] J. Benoy and R. N. Kale, “Condensate stabilization,” *Offshore World*, pp. 34–37, 2010.

[9] N. Moghadam, M. Samadi, and Z. B. Hosseini,

"Simulation of Gas Condensate Stabilization Unit Aiming at Selecting the Right Technique and Assessing the Optimized Operational Parameters," in *International Conference on Chemical, Biological and Environmental Engineering*, 2012.

[10] N. Tahouni, R. Khoshchehreh, and M. H. Panjeshahi, "Debottlenecking of condensate stabilization unit in a gas refinery," *Energy*, vol. 77, pp. 742–751, 2014.

[11] M. H. Salimi and T. Zarei, "Heat integration of the gas condensate stabilization unit, a case study from the south pars gas field in the Persian Gulf," *European Journal of Technology and Design*, vol. 9, no. 3, pp. 107–114, 2015.

[12] N. Rahmanian, L. S. B. Jusoh, M. Homayoonfard, K. Nasrifar, and M. Moshfeghian, "Simulation and optimization of a condensate stabilisation process," *J Nat Gas Sci Eng*, vol. 32, pp. 453–464, 2016.

[13] H. Uwitonze, K. S. Hwang, and I. Lee, "Modelling and improving natural gas condensate process with stripping and heat integration," *Chemical Engineering and Processing: Process Intensification*, vol. 118, pp. 71–77, 2017.

[14] M. Bahmani, J. Shariati, and A. N. Rouzbahani, "Simulation and optimization of an industrial gas condensate stabilization unit to modify LPG and NGL production with minimizing CO2 emission to the environment," *Chin J Chem Eng*, vol. 25, no. 3, pp. 338–346, 2017.

[15] A. Hajizadeh, F. Mirghaderi, R. Azin, and H. Rajaei, "Optimization and energy efficiency investigation of an industrial gas condensate separation plant," in *16th International Conference on Clean Energy (ICCE-2018)*, 2018.

[16] A. Hajizadeh *et al.*, "Improvement of Energy Efficiency in Gas Condensate Stabilization Unit: Process Optimization Through Exergy Analysis," in *SPE Canadian Energy Technology Conference*, OnePetro, 2022.

[17] D. C. Y. Foo, Z. A. Manan, M. Selvan, and M. L. McGuire, "Integrate process simulation and process synthesis," *Chem Eng Prog*, vol. 101, no. 10, pp. 25–29, 2005.

[18] I. D. G. Chaves, J. R. G. López, J. L. G. Zapata, A. L. Robayo, and G. R. Niño, *Process analysis and simulation in chemical engineering*. Springer, 2016.

[19] S. A. Junior, A. P. Meneguelo, L. Arrieche, and M. Bacelos, "Assessment of a process flow diagram for NGL recovery using different condensation mechanisms," *Comput Chem Eng*, vol. 130, p. 106557, 2019.

[20] H. Al-Ali, "Process simulation for crude oil stabilization by using Aspen Hysys," *Upstream Oil and Gas Technology*, vol. 7, p. 100039, 2021.

[21] Z. Yuan, M. Cui, R. Song, and Y. Xie, "Evaluation of prediction models for the physical parameters in natural gas liquefaction processes," *J Nat Gas Sci Eng*, vol. 27, pp. 876–886, 2015.

[22] Y. Jung, N. V. D. Long, M. G. Woldetensay, and M. Lee, "A Study of Complex Distillation Arrangements for Improved Depropanizing, Debutanizing and Deisobutanizing Fractionation of NGL," in *Computer Aided Chemical Engineering*, Elsevier, 2012, pp. 680–684.

[23] A. Tamuzi, N. Kasiri, and A. Khalili-Garakani, "Design and optimization of distillation column sequencing for NGL fractionation processes," *J Nat Gas Sci Eng*, vol. 76, p. 103180, 2020.

[24] M. M. El-Eishy, G. M. Abdelalim, and T. M. Aboul-Fotouh, "SIMULATION STUDY AND OPTIMIZATION OF THE OPERATING VARIABLES AFFECTING THE PERFORMANCE OF AN EXISTING CONDENSATE STABILIZATION UNIT.," *Petroleum & Coal*, vol. 61, no. 6, 2019.

[25] M. J. Guerra, "Aspen HYSYS property packages overview and best practices for optimum simulations," *Aspen Process Engineering Webinar*, 2006.

[26] M. M. Fard, F. Pourfayaz, A. B. Kasaeian, and M. Mehrpooya, "A practical approach to heat exchanger network design in a complex natural gas refinery," *J Nat Gas Sci Eng*, vol. 40, pp. 141–158, 2017.

[27] M. Shamsi, E. Naeiji, S. Moghaddas, and M. M. Sheidaei, "Techno-Economic, Energy, Exergy, and Environmental (4e) Analysis for a New Integrated Post-Combustion Co2 Capture Process".

[28] T. B. H. Nguyen and E. Zondervan, "Methanol production from captured CO2 using hydrogenation and reforming technologies_ environmental and economic evaluation," *Journal of CO2 utilization*, vol. 34, pp. 1–11, 2019.

[29] C. Nwaoha, M. Beaulieu, P. Tontiwachwuthikul, and M. D. Gibson, "Techno-economic analysis of CO2 capture from a 1.2 million MTPA cement plant using AMP-PZ-MEA blend," *International Journal of Greenhouse Gas Control*, vol. 78, pp. 400–412, 2018.

[30] O. Y. Abdelaziz, W. M. Hosny, M. A. Gadalla, F. H. Ashour, I. A. Ashour, and C. P. Hulteberg, "Novel process technologies for conversion of carbon dioxide from industrial flue gas streams into methanol," *Journal of CO2 utilization*, vol. 21, pp. 52–63, 2017.